Multilayer Growth of Porphyrin-Based Polyurea Thin Film Using Solution-Based Molecular Layer Deposition Technique

S. M. Nizam Uddin[†], Yuki Nagao[†*]

[†]*School of Materials Science, Japan Advanced Institute of Science and Technology, 1-1 Asahidai, Nomi, Ishikawa 923-1292, Japan*

Abstract

Controllable synthesis of organic thin film materials on solid surfaces is a challenging issue in the research field of surface science as it is affected by several physical parameters. In this work, we demonstrated a solution-based molecular layer deposition (MLD) approach to prepare porphyrin-based covalent organic molecular networks on a 3-aminopropyl trimethoxysilane (APTMS) modified substrate surface using the urea coupling reaction between 1,4-phenylene diisocyanate (1,4-PDI) and 5,10,15,20-tetrakis-(4-aminophenyl) porphyrin (H_2TAPP) at room temperature (22 ± 2 ºC). Multilayer growth was investigated under different relative humidity (RH) conditions of the reaction chamber. Sequential molecular growth at low relative humidity (≤10% RH) was observed using UV-vis absorption spectroscopy and atomic force microscopy (AFM). The high-RH condition shows limited film growth. Infrared spectroscopy (IR) and X-ray photoelectron spectroscopy (XPS) revealed the polyurea bond formation in sequential multilayer thin films, demonstrating that stepwise multilayer film growth was achieved using the urea coupling reaction.

Introduction

Fabrication of functionalized organic thin films has become a burgeoning area in the research field of surface science over the last few decades.[1-4] Scientists from different backgrounds have introduced versatile new methods for thin film synthesis using top-down and bottom-up approaches.[5-6] Bottom-up approach offers an opportunity to synthesize the nanostructure on the substrate surface by stacking the atoms and/or molecules on each other with less defects, homogenous chemical composition and better short- and long-range ordering.[6-8] Bottom-up approach includes the various thin film fabrication techniques such as Layer-by-layer (LbL),[9] Langmuir-Blodgett (LB),[10-11] spin coating,[12] microwave[13] and electrochemical deposition.[14] Among all of these, molecular level LbL thin film fabrication known as molecular layer deposition (MLD) has gained an extensive attention in today's research world because of its simplicity and its attractive control over film thickness, composition, and conformality through sequential self-limiting surface reaction at the single-molecule level.[15-18] As covalently bonded films possess much higher chemical and thermal stability (because of their chemical characteristics)[19-21] compared to the conventional MLD film fabrication based on non-covalent interactions such as coulombic interactions[22-23] and hydrogen bonding.[24] To date, most MLD processes have been conducted through polymerization of volatile bifunctional monomers under vacuum conditions to prepare polyamide,[25-27] polyimide,[28-29] polyurethane,[30] and polyurea[15,31-32] based nanostructures. The urea coupling reaction offers a significant benefit to avoid the byproduct entrapment within the polymer film as no byproduct is produced in this reaction process.[15,26] In addition, the interlayer linking functionality of urea moiety has the ability to form hydrogen-bonded network that helps to form molecular network on the substrate surface.[33] The use of urea functionalities to enhance the stability in aromatic supramolecular structures is also well-known because of their hydrogen-bonding ability between adjacent urea groups along with the π–π stacking

interaction between neighboring aromatic building blocks. Several research groups including Bent[34-36] and Blanchard[33] have utilized bifunctional monomers to fabricate polyurea thin films including interlayer hydrogen-bonding between adjacent urea groups. Park and co-workers reported a multilayer polyurea thin film using same symmetrical tetrafunctional monomers.[37] Recently, our research group has demonstrated a cross-linked polyurea thin film using a different symmetrical bifunctional and tetrafunctional monomers.[15]

In this work, the solution-based MLD technique is chosen to establish porphyrin-based covalent organic thin film through the urea coupling reaction between bifunctional 1,4-phenylene diisocyanate (1,4-PDI) and tetrafunctional 5,10,15,20-tetrakis-(4-aminophynyl) porphyrin (H_2TAPP) monomers (Scheme 1). The choice of these monomers was based on their chromophore properties in the multilayer thin film and commercial availability. Two different wavelength regions of phenylurea and porphyrin in UV-vis absorption spectroscopy assisted to investigate the multilayer film growth at different RH conditions of the reaction chamber. The main focus of this paper is on demonstrating the use of conventional isocyanate-amine chemistry to fabricate porphyrin-based polyurea multilayer assemblies. Systematic characterization of the sequential molecular growth was accomplished using UV-vis absorption spectroscopy and atomic force microscopy (AFM). Moreover, chemical characteristics of the multilayer organic thin film were characterized using infrared spectroscopy (IR) and X-ray photoelectron spectroscopy (XPS).

Scheme 1. Schematic representation of MLD process to fabricate porphyrin-based multilayer thin film

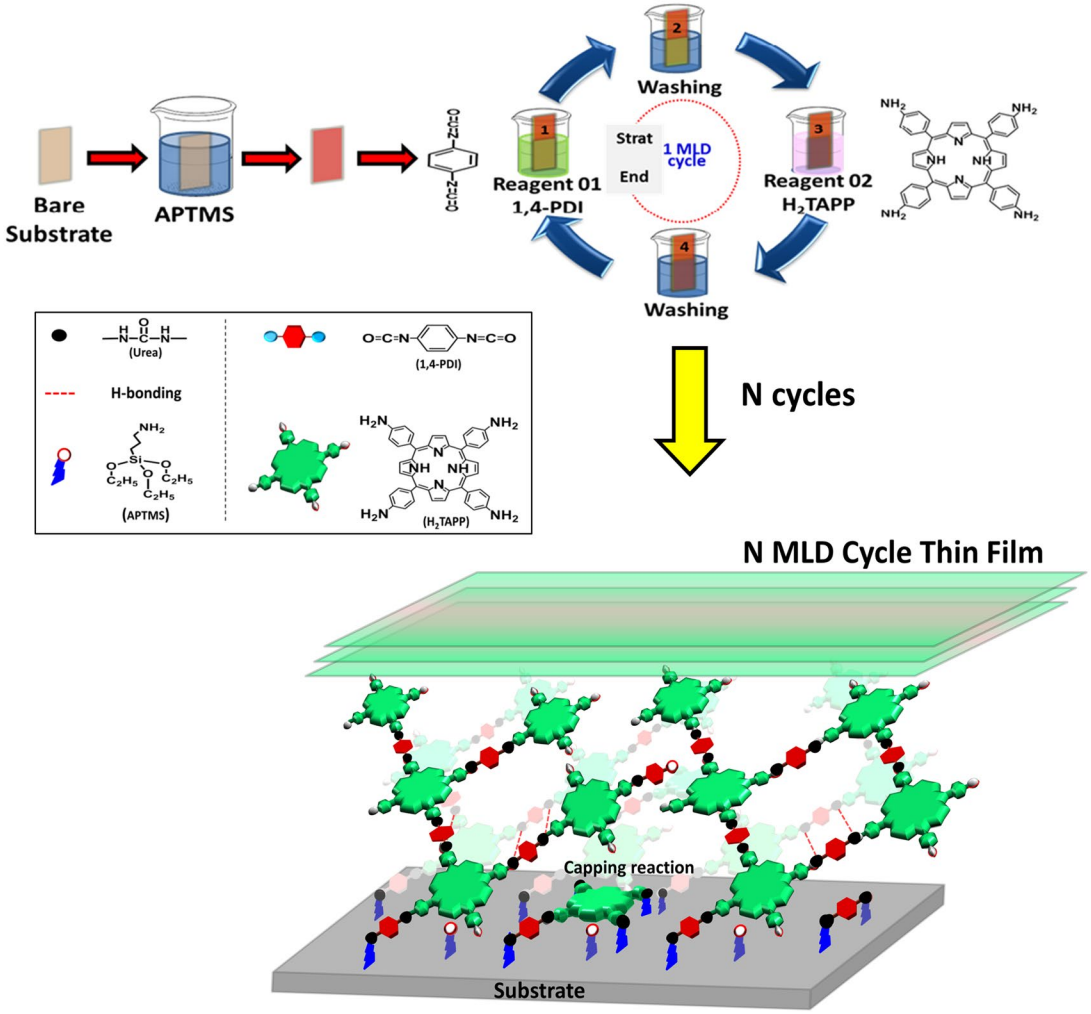

Experimental

Materials

Silicon wafer (Si (100), p-type) and quartz (SiO_2) substrates were purchased from Electronics and Materials Corp. Ltd. and Sendai Sekiei Glass Seisakusho respectively. 5,10,15,20-tetrakis-(4-aminophynyl) porphyrin (H_2TAPP, >95%), 1,4-phenylene diisocyanate (1,4-PDI, >98%) and 3-aminopropyltri methoxysilane (APTMS, >96%) were purchased from Tokyo Chemical Industry Co. Ltd., Japan. Before use, 1,4-PDI was further purified by sublimation. HPLC (99.7%) grade of ethanol and 2-propanol was used for substrate modification with APTMS. Super dehydrated (H_2O, $\leq$0.001%) chloroform ($CHCl_3$), tetrahydrofuran (THF), toluene and N, N-dimethylformamide (DMF) were used for the formation of multilayer thin films. All solvents were purchased from Wako Pure Chemical Industries Ltd., Japan, and were used as-received without further purification.

Modification of Solid Substrate with APTMS

SiO_2 (25 × 15 mm^2, t = 0.5 mm) and Si (30 × 20 mm^2, t = 0.5 mm) substrates were cleaned by sonication for 3 × 15 min using 2-propanol (HPLC grade, 99.7%) to remove organic contaminants. To obtain the amine-functionalized self-assembled monolayers (SAMs), clean SiO_2 and Si substrates were immersed into 10 mM ethanol solution of APTMS for 1 hr with mild shaking at room temperature (22 ± 2 ºC) under an Ar atmosphere. After taking out from the APTMS solution, the substrates were washed with HPLC grade (99.7%) of ethanol (twice) and 2-propanol (twice) consecutively with sonication for 5 min each, and were finally rinsed with 2-propanol and dried with an Ar stream in a clean bench. Characterizations of the APTMS-modified substrate are shown in Figures S1–S3.

Fabrication of Multilayer Thin Film on Modified Solid Substrate

Amine-functionalized substrates were used for the fabrication of multilayer thin films in a RH controlled chamber at different relative humidity (RH) condition. The RH of the reaction chamber was controlled by using Ar gas flow and monitored by RH sensor. Fabrication of multilayer thin film was carried out in super dehydrate solvents (H_2O, ≤0.001%) at room temperature with the following steps: (i) the amine-functionalized substrate was immersed into 4.4 mM 1,4–PDI in the mixture solvent of $CHCl_3$ and THF (8:2, v/v) for 25 min. Then the substrate was rinsed successively with two beakers of toluene and two beakers of THF separately for each 2 min washing. (ii) The resulting isocyanate functionalized substrate was immersed into 1.5×10^{-1} mM H_2TAPP in the mixture solvent of $CHCl_3$ and THF (8:2, v/v) for 25 min, with subsequent washing successively using two beakers of DMF and two beakers of THF separately for each 2 min washing to remove the unreacted precursors onto the deposited film and dried under Ar atmosphere. This bilayer deposition obtained from step (i) and (ii) was regarded as the 1 MLD cycle. The steps described above were repeated to fabricate the multilayer films used for characterization.

Characterization

UV-vis absorption spectra of the multilayer thin film deposited on the SiO_2 substrates were measured using a UV-vis spectrometer (Jasco V-630BIO-IM; Jasco Corp., Japan). The APTMS-modified SiO_2 substrate was used as a reference sample. Transmission Fourier transform infrared (FTIR) was used to characterize the MLD film formation. IR spectra were collected with a Fourier transform infrared (FTIR) spectrometer (Nicolet 6700, Thermo Fisher Scientific Inc.) equipped with a mercury cadmium telluride (MCT) detector. An APTMS-modified Si substrate was used as a reference sample. The signal noise has been subtracted by smoothing process. Tapping mode atomic force microscopy (AFM) was used to

analyze the film surface morphology and roughness. AFM images were collected using a digital AFM system (NanoScope IIIa; Veeco Instruments). Silicon probes were used as a cantilever (SI-DF3FM; Nanosensors Corp.) with a resonance frequency of 60-66 kHz and a spring constant of 2.8–4.4 N/m. The measurements were taken under an air atmosphere with a scan rate of 0.4 Hz and scan sizes of 500 nm × 500 nm and 1 μm × 1 μm. Multilayer film thickness was measured using AFM (VN-8000; Keyence Co.) equipped with a DFM/SS mode cantilever (OP-75041; Keyence Co.) and white interference microscope (BW-S506, Nikon Co.). For thickness measurement, samples were prepared by covering a portion of bare substrate with thin Au coating followed by APTMS and multilayer thin film formation. Finally the thin Au coated portion was carefully removed from the substrate surface by using cotton bar before thickness measurements. Measurements were taken at four different positions, at least, to estimate the average film thickness. The thickness of APTMS-modified substrate was used as a baseline thickness, which was subtracted from the subsequent film thickness of the multilayer thin film includes APTMS. To confirm the elemental characteristics of the thin films, X-ray photoelectron spectroscopy (XPS) study was performed using a DLD spectrometer (Kratos Axis-Ultra; Kratos Analytical Ltd.) with an Al Kα radiation source (1486.6 eV). Energy and component separations were conducted using bundled vision processing software with pure Gaussian profiles with a Shirley background.

Results and Discussion

To achieve controlled film growth throughout the deposition process, optimized reaction conditions such as monomer concentration, immersion time, and physisorption were ascertained carefully as shown in Figures S4–S6. For this work, moisture-sensitive 1,4-PDI (containing isocyanate group) was used as one precursor,[33,37] which may have different degrees of self-polymerization with respect to RH conditions of the reaction chamber. Considering this issue, the effect of RH on film growth was investigated using UV-vis absorption spectroscopy. Figure 1 depicts the UV-vis absorption spectra of 1 MLD cycle films as a function of RH condition of the reaction chamber. The absorbance increased significantly at 260 nm and decreased at 430 nm from 54 ± 2% to 10 ± 2% RH of the reaction chamber. But the absorbance remains almost same in the cases of 5 ± 2% and 10 ± 2% RH, representing a tentative RH condition for the fabrication of porphyrin-based polyurea thin film. The higher number of phenylurea formation (at 260 nm)[15,33,38] at high–RH reduced the reaction possibilities of porphyrin precursors. At high RH condition of the reaction chamber, hydrolysis of isocyanate group is expected to form the corresponding carbamic acid at the

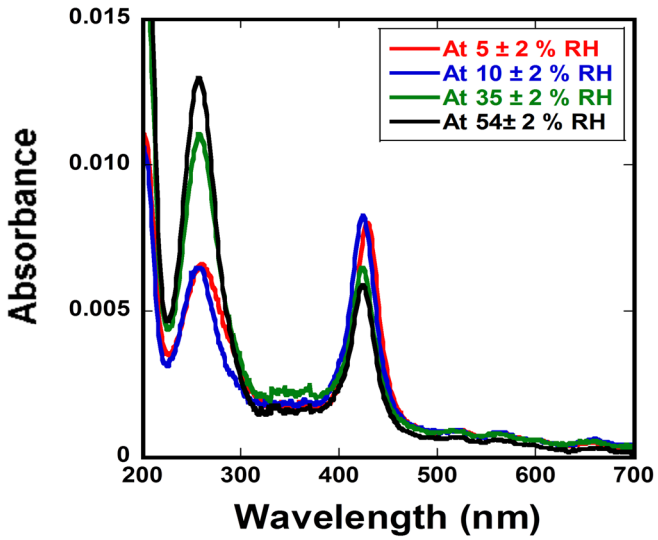

Figure 1. UV-vis absorption spectra of 1 MLD cycle films on the quartz slides as a function of RH condition of the reaction chamber (immersion time = 25 min/0.5 MLD cycle).

presence of water vapor that might be converted to amine with the evolution of carbon dioxide.[33] Thus, another isocyanate group containing 1,4-PDI molecule can react with the carbamic acid intermediate or amine to form corresponding urea as the final product of self-polymerization (Scheme 2).[33] As a consequence the top surface of the film could be blocked by the self-polymerization of 1,4-PDI molecules. These might reduce the availability of isocyanate groups that is required for the molecular growth of H_2TAPP through the urea coupling reaction (Scheme 3).

Scheme 2. Hydrolysis of isocyanate group to form a carbamic acid (intermediate) and the subsequent decomposition to produce amine, leading self-polymerization of 1,4-PDI molecules

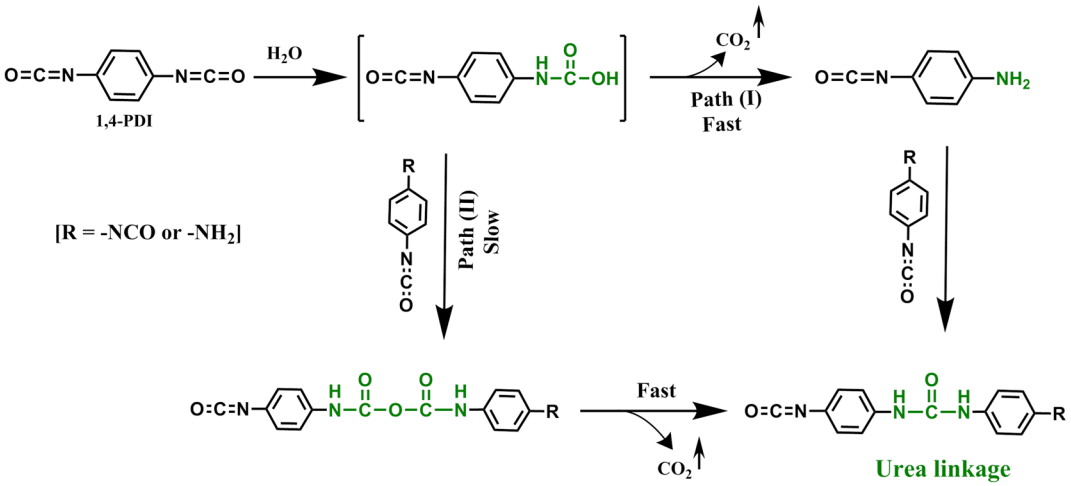

Scheme 3. Reaction between isocyanate and amine group to form urea linkage

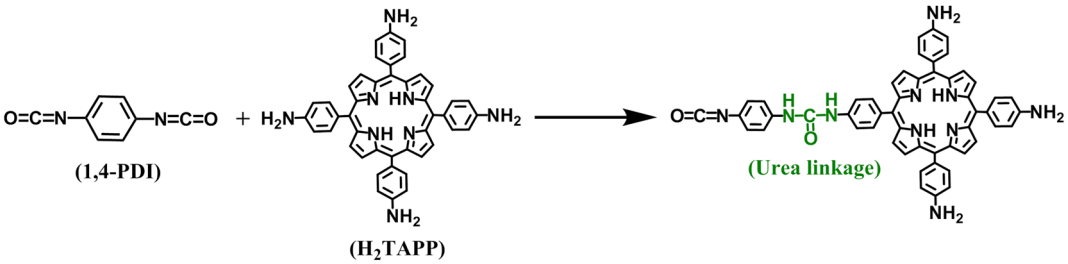

For clarification, XPS spectra of 1 MLD cycle films were taken at both low (10 ± 2%) and high (34 ± 2%) RH conditions of the reaction chamber. The N 1s XPS fine scan spectra showed that the peak area of urea response prepared at the high–RH condition is 70% larger than the film prepared at the low–RH condition. The characteristic iminic (=N-) and pyrrolic (N–H) peak areas of porphyrin showed 10% lower response from low to high RH conditions (Figure S7). That can only occur when 1,4-PDI becomes self-polymerized at the high–RH condition. Figure 2 portrays the continuous increase of absorbance as a function of MLD cycles at 10 ± 2% RH of the reaction chamber, indicating stepwise film growth.[15,37,39] Stepwise film growth at 10 ± 2% RH shows almost similar tends with 5 ± 2% RH condition (Figure S8a). However, limiting film growth was observed in a high–RH condition (Figure S8b). These results signify that, at high RH, a considerable amount of 1,4-PDI self-polymerization blocks the reactive surface sites that leads to a lower accessibility of the porphyrin molecules for molecular growth.[25,34] During multilayer film growth, 1 MLD cycle film showed higher absorbance at 260 nm compared to the growth sequence of following

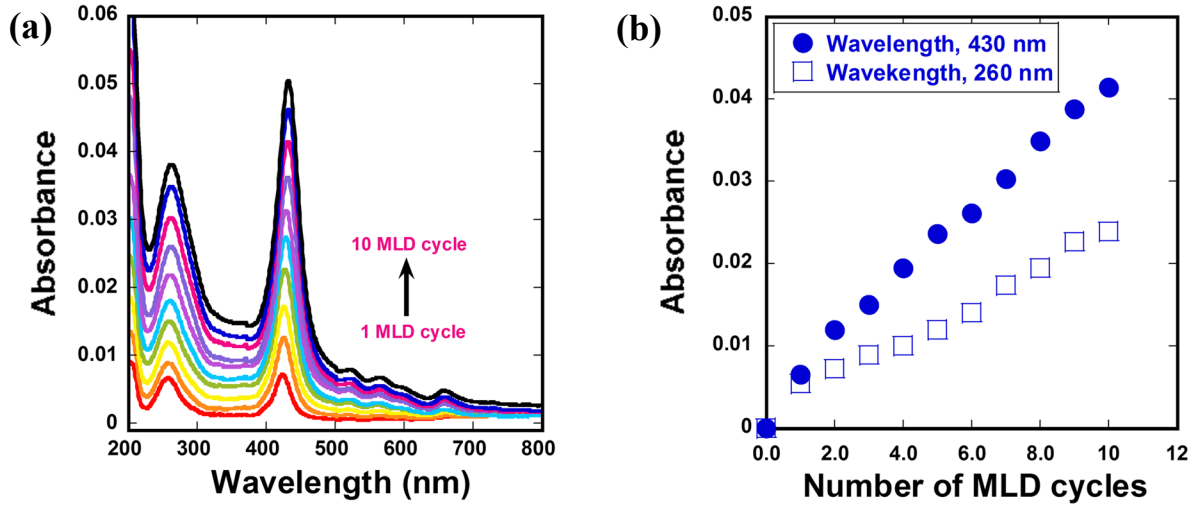

Figure 2. (a) UV-vis spectra of multilayer thin film as a function of MLD cycles on APTMS-modified quartz slides and (b) linear plot of absorption intensity vs. the number of MLD cycles at 10 ± 2 % RH of the reaction chamber.

MLD cycles. It might have occurred as a result of capped region caused by the double reaction of 1,4-PDI precursors because the molecular population is largest at the initial steps of film growth.[18,40]

To demonstrate the growth behavior, thickness of 2, 5, 8, and 10 MLD cycle thin films were investigated using AFM and white interference microscope (Figure S9). Figure 3 depicts the sequential growth behavior with the number of MLD cycles, confirming stepwise film formation at10 ± 2 % RH of the reaction chamber.[18,23] The film growth rate for 1,4-PDI/H_2TAPP film was found to be approximately 0.80 ± 0.03 nm/MLD cycle. The thickness of AFM results are well matched to the white interference microscope results. This growth rate is lower than the combined molecular length of 1,4-PDI and H_2TAPP molecules, which is estimated as approximately 2.08 nm, based on the constituent bond length of 1,4-PDI and H_2TAPP molecules. Deviation of the growth rate can be attributed to several factors. First, the film growth direction is not perpendicular to the substrate surface. In fact, the tilted configuration of MLD film with respect to the surface might dominate the structure.[35] It is expected that the multilayer films are growing at an average angle of 64° from the substrate

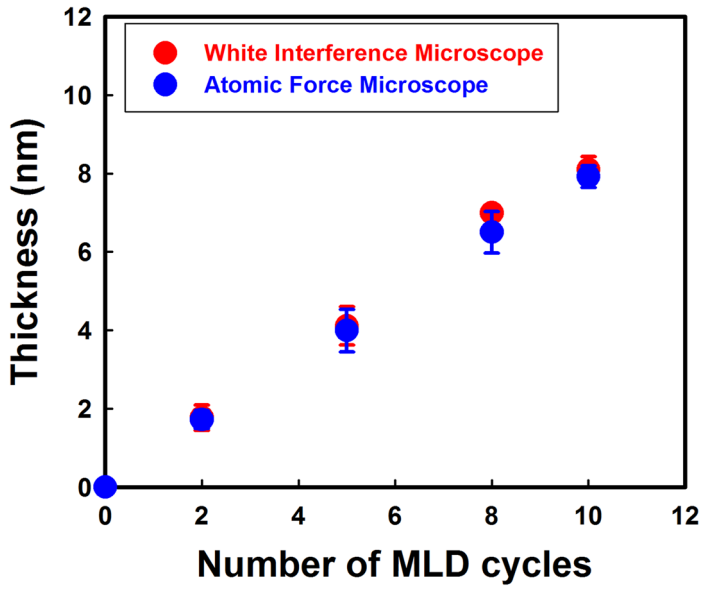

Figure 3. Film thickness as a function of number of MLD cycles prepared at 10 ± 2 % RH of the reaction chamber.

surface normal. Second, a fraction of incident precursors may react with the reactive film surface to form a capped region.[18,34]

From the discussion presented above, it was not confirmed that the multilayer film growth occurred by a urea coupling reaction between isocyanate and amine groups. Therefore, IR spectroscopic measurements were taken to investigate chemical bonding into the molecular films. Figure 4 presents the IR spectra for 5 and 10 MLD cycle thin films. Several characteristic peaks were observed in the IR fingerprint region. The band around 1635 and 1670 cm^{-1} can be assigned as amide I band resulting from the H-bonded and free υ(C=O) stretching vibration mode of urea group respectively. The amide II band as δ(N–H) bending vibration was observed around 1510 cm^{-1}. Peaks around 1311 and 1180 cm^{-1} can be assigned for the asymmetric υ_{as}(N–C–N) and symmetric υ_{s}(N–C–N) stretching modes respectively. All characteristic peaks confirmed the formation of urea linkage.[15,33,35-36,41] In addition, the out-of-plane γ(N–H) vibration of pyrrole in free-base porphyrin was observed at around 730 and 800 cm^{-1}. A shoulder type υ(N–H) band was also observed at around 965 cm^{-1} for in-plane N–H vibration of pyrrole.[42-43] Furthermore, the absorbance increased with the number of MLD

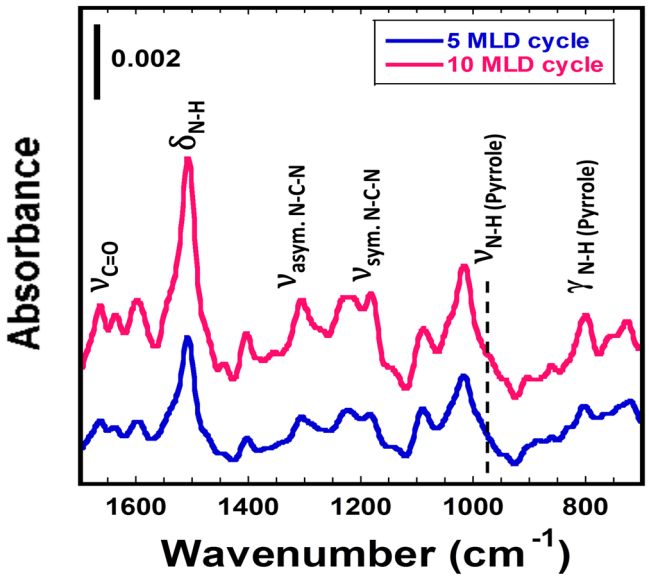

Figure 4. IR spectra of 5 and 10 MLD cycle thin films on the APTMS-modified Si substrates.

cycles, reflecting that the polyurea-based growth behavior occurred along with the multilayer film formation. No peak was observed at around 2270 cm^{-1} for υ_{as}(N=C=O) stretching,[36] indicating the absence of unreacted isocyanate groups in the films (Figure S10).

For further characterization, XPS was used to explore the chemical characteristics of the molecular networks. Elemental fine scan spectra revealed the atomic environment and chemical bonding in the multilayer thin film (Figure 5a–5c). The N 1s XPS fine scan spectra for 10 MLD cycle film showed five different types of components (Figure 5a). The main

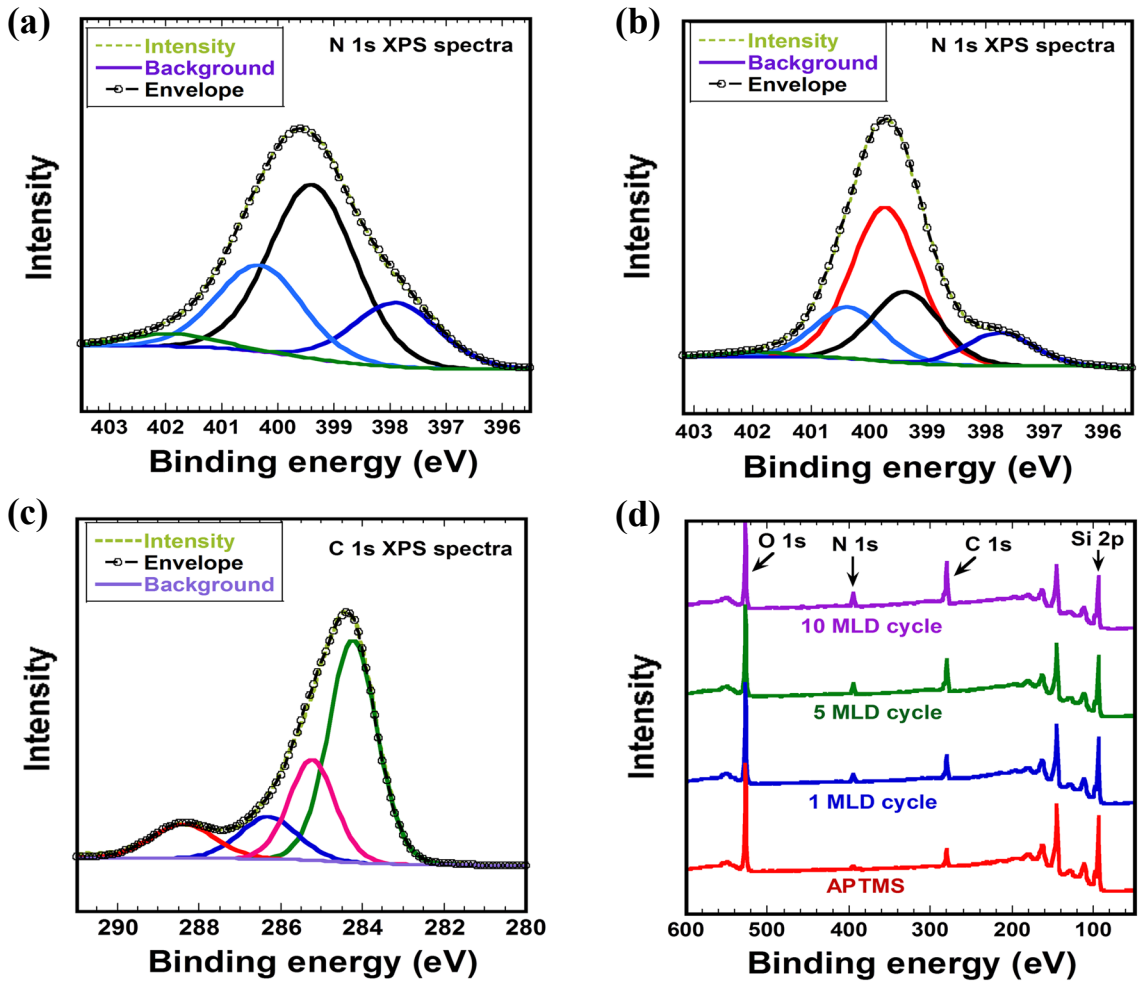

Figure 5. N 1s XPS fine scan spectra for (a) H_2TAPP powder and (b) 10 MLD cycle film. (c) C 1s XPS fine scan spectra for 10 MLD cycle thin film and (d) XPS survey spectrum for APTMS, 1 MLD, 5 MLD, and 10 MLD cycle thin films.

peak at 399.8 eV represents the urea (O=C–N–H) groups.[15,35,37] The lowest binding energy peak at 397.9 eV and higher binding energy peak at 400.4 eV correspond to the iminic (=N-) and pyrrolic (N–H) groups respectively.[47] The intermediate binding energy peak at 399.4 eV resulted from the non-hydrogen bonded free amine (NH_2).[15,44-45] Finally, the minor peak at the higher binding energy around 401.9 eV represents the hydrogen bonded amine and nitrogen shakeup satellite of porphyrin.[44-45] The binding energies of N 1s XPS fine scan spectra for 10 MLD cycle film showed good matching with the N 1s XPS fine scan spectra for H_2TAPP powder, as shown in Table 1.

Table 1. Peak assignments of the N 1s XPS fine scan spectra for H_2TAPP powder and 10 MLD cycle films

Sample	=N- (Iminic)	Free NH_2	N–H (Pyrrolic)	H-bonded NH_2 / N-shakeup satellite	O=C–N–H
H_2TAPP powder	397.9 eV	399.4 eV	400.4 eV	401.9 eV	-
10 MLD cycle film	397.9 eV	399.4 eV	400.4 eV	401.9 eV	399.8 eV

Consideration of the peak area ratio of the deconvoluted N-components revealed that the urea (O=C–N–H) and free amine (NH_2) responses are 3.2 and 1.3 times higher than the pyrrolic (N–H) group respectively. Indicating that, on average, only 2–3 amine groups of each porphyrin molecule took part in the reaction during stepwise film growth. Some additional urea and free amines might be observed because of the capping reaction of incident precursors[34] and unreacted amine and isocyanate groups which were easily converted to amine by humid air. In addition, C 1s XPS spectra for 10 MLD cycle film showed four

components (Figure 5c). The lowest binding energy peak at 284.5 eV is attributed to the aromatic carbon (C=C) and C–H bonds.[15] The highest binding energy peak at 288.5 eV corresponds to the carbonyl (C=O) group of urea linkage.[15,45] And the intermediate binding energy peaks at 285.7 eV and 286.5 eV denote the sp^2 C–N and C=N bond respectively.[45] No isocyanate peak was observed from N 1s and C 1s XPS fine scan spectra.[46] These assignments of N 1s and C 1s XPS fine scan spectra are consistent with IR results and were previously reported polyurea-based works.[15,33-37,41,44-45] All results confirmed the urea bond formation consistently into the multilayer thin film. Figure 5d presents survey spectra of APTMS, 1 MLD, 5 MLD, and 10 MLD cycle thin films. Results show that N 1s and C 1s peak intensities increase concomitantly with decreasing Si 2p peak intensity from APTMS to 10 MLD cycle thin films, indicating that the multilayer film covers the Si/SiO_2 surface. Additionally, it is noteworthy that N 1s peak intensity for 1 MLD cycle film is higher than the calculated one MLD cycle of 5 and 10 MLD cycle thin films. That result might have occurred due to the presence of unreacted amine-functionalized APTMS (H-bonded amine)[45] and the capped region caused by the double reaction of 1,4-PDI or H_2TAPP precursors because the molecular population is larger at the initial steps of film growth.[18,34] These results are relevant with the observation of UV-vis absorption response for multilayer film growth (Figure 2).

The topography of SiO_2-supported polyurea thin films was also investigated using tapping mode AFM, as shown in Figure 6. The 2D and 3D AFM height images of 5 and 10 MLD cycle thin films show homogeneous surface within 500 nm × 500 nm area, which indicates the well deposition process. It was made up of numerous small grain-like domains along the horizontal axis with the diameter of *ca.* 10–20 nm, which increases slightly from 5 to 10 MLD cycle thin films. The root mean square (RMS) roughness was also investigated; where roughness increased from 0.36 to 0.48 nm for 5 and 10 MLD cycle thin films respectively. In comparison to the bare SiO_2 substrate and APTMS-modified SiO_2 substrate, 5 and 10 MLD

cycle films show greater domain size and RMS roughness (Figure S11), which signifies the molecular layer growth on the APTMS-modified Si substrate.[15,23]

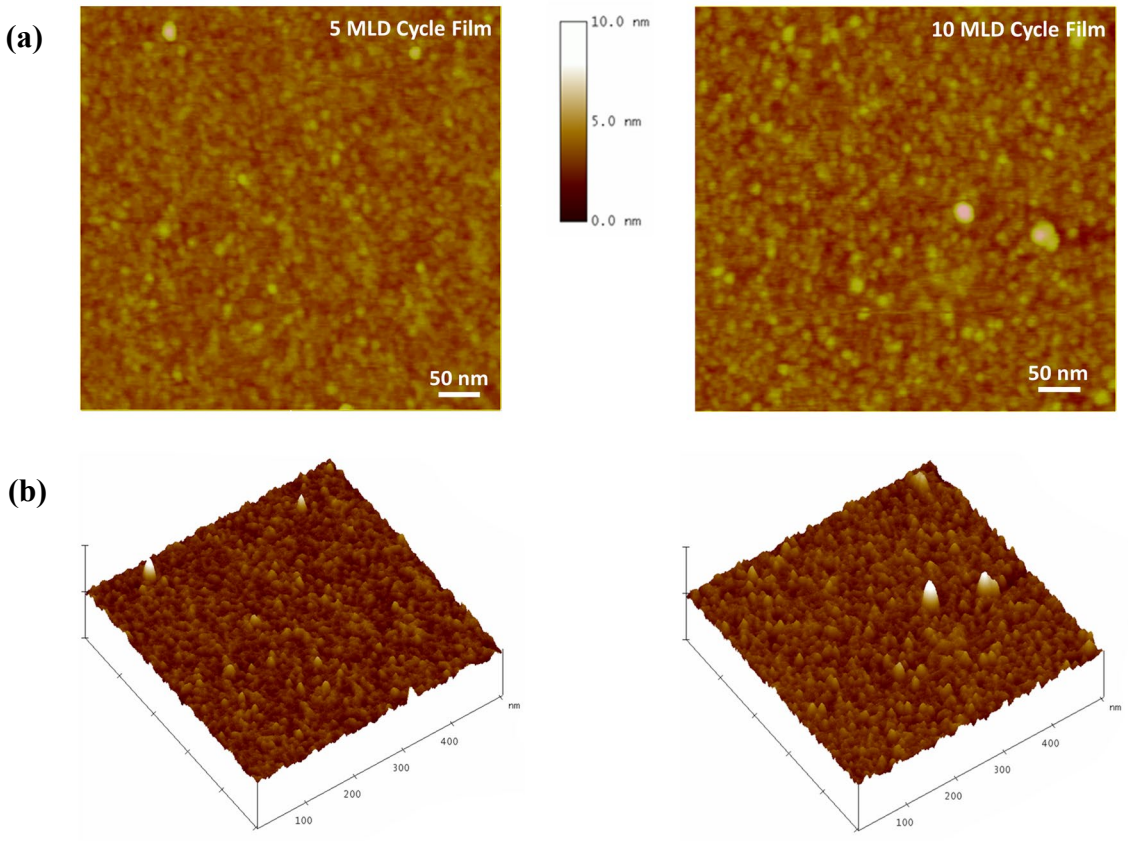

Figure 6. (a) 2D and (b) 3D AFM height images of 5 MLD and 10 MLD cycle thin films. Scan size: 500 nm × 500 nm. Data scale 10 nm.

In this covalent network system, results suggest that the humidity at 10 ± 2% RH could be an acceptable condition for the achievement of porphyrin-based polyurea multilayer thin film networks on solid surface.

Conclusions

We have demonstrated the solution-based MLD thin film growth of porphyrin-based covalent molecular networks on a APTMS-modified substrate surface using the urea coupling reaction between 1,4-PDI and H_2TAPP at room temperature. UV-vis absorption spectra showed stepwise multilayer film growth at ≤10% RH condition of the reaction chamber, whereas the

high RH condition showed film growth-limiting behavior. Presumably, numerous 1,4-PDI self-polymerization took place at high RH conditions. This might block the reactive surface area that leads to a lower accessibility of porphyrin molecules for multilayer film growth. White interference microscope confirms the film thickness measured by AFM and indicates that the multilayer films prepared at 10 ± 2% RH of the reaction chamber are growing at an average angle of 64° relative to the substrate surface normal. FTIR spectra of multilayer thin films showed four characteristic IR vibrational bands for urea linkage along with the in-plane and out-of-plane vibrational modes of pyrrole from metal free porphyrin. The IR responses at around 1635 and 1670 cm^{-1} confirmed the presences of hydrogen bonded and free urea respectively into the multilayer thin film. The IR signal also increased significantly with the number of MLD cycles, representing the sequential multilayer film growth caused by consecutive urea coupling reaction. Furthermore, deconvoluted high resolution N 1s and C 1s XPS fine scale spectra represent an additional evidence of urea bond formation into the multilayer thin films. Peak area ratio of the deconvoluted N-component revealed that, on average, only 2-3 amine groups of each porphyrin molecule took part in the urea coupling reaction for multilayer film formation.

ASSOCIATED CONTENT

Supporting Information

UV-vis, IR, XPS, white interference microscope and AFM studies of substrate surface-modification and MLD cycle thin film formation. This materials is available free of charge via the Internet at http://pubs.acs.org.

AUTHOR INFORMATION

Corresponding Author

*ynagao@jaist.ac.jp Phone: +81(Japan)-761-51-1541, Fax: +81(Japan)-761-51-1149

Notes

The authors declare no competing financial interest.

ACKNOWLEDGMENTS

The authors thank Dr. Md. A. Rashed and Dr. Salinthip Laokroekkiat for their advice and technical assistances. This work was financially supported by The Murata Science Foundation, Japan.

References

(1) DiBenedetto, S. A.; Facchetti, A.; Ratner, M. A.; Marks, T. J. Molecular Self-Assembled Monolayers and Multilayers for Organic and Unconventional Inorganic Thin-Film Transistor Applications. *Adv. Mater*. **2009**, *21*, 1407.

(2) Roberts, M. E.; Sokolov, A. N.; Bao, Z. Material and device considerations for organic thin-film transistor sensors. *J. Mater. Chem.* **2009**, *19*, 3351–3363.

(3) Nakazawa, M.; Kosugi, T.; Nagatsuka, H.; Maezawa, A.; Nakamura, K.; Ueha, S. Polyurea Thin Film Ultrasonic Transducers for Nondestructive Testing and Medical Imaging. *IEEE Trans.* **2007**, *54*, 2165–2174.

(4) Evans-Nguyen, K. M.; Tolles, L. R.; Gorkun, O. V.; Lord, S. T.; Schoenfisch, M. H. Interactions of Thrombin with Fibrinogen Adsorbed on Methyl-, Hydroxyl-, Amine-, and Carboxyl-Terminated Self-Assembled Monolayers. *Biochemistry* **2005**, *44*, 15561–15568.

(5) Wang ZM: One-Dimensional Nanostructures. Springer Science + Business Media, LLC, 233 Spring Street, New York, NY 10013, USA: Springer **2008**.

(6) Teo, B. K.; Sun, X. H. From Top-Down to Bottom-Up to Hybrid Nanotechnologies: Road to Nanodevices. *J. Cluster Sci.* **2006**, *17*, 529-540.

(7) Foo, K. L.; Hashim, U.; Muhammad, K.; Voon, C. H. Sol–gel synthesized zinc oxide nanorods and their structural and optical investigation for optoelectronic application. *Nanoscale Res. Lett*. **2014**, *9*, 429.

(8) Cao, G. Z.; Wang, Y. Nanostructures and Nanomaterials: Synthesis, Properties, and Applications. 2nd edition. Singapore 596224: World Scientific Publishing Co. Pte. Ltd. **2010.**

(9) Zacher, D.; Yusenko, K.; Bétard, A.; Henke, S.; Molon, M.; Ladnorg, T.; Shekhah, O.; Schüpbach, B.; de los Arcos, T.; Krasnopolski, M.; Meilikhov, M.; Winter, J.; Terfort, A.; Wöll, C.; Fischer, R. A. Liquid-Phase Epitaxy of Multicomponent Layer-Based Porous Coordination Polymer Thin Films of [M(L)(P)0.5] Type: Importance of Deposition Sequence on the Oriented Growth. *Chem. Eur. J.* **2011**, *17*, 1448–1455.

(10) Gole, A.; Jana, N. R.; Selvan, S. T.; Ying, J. Y. Langmuir-Blodgett Thin Films of Quantum Dots: Synthesis, Surface Modification, and Fluorescence Resonance Energy Transfer (FRET) Studies. *Langmuir* **2008,** *24,* 8181–8186.

(11) Choudhury, S.; Betty, C. A.; Bhattacharyya, K.; Saxena, V.; Bhattacharya, D. Nano-structured PdO Thin Film from Langmuir−Blodgett Precursor for Room-Temperature H_2 Gas Sensing. *ACS Appl. Mater. Interfaces* **2016**, *8*, 16997−17003.

(12) Seon, J-B.; Lee, S.; Kim, J. M. Spin-Coated CdS Thin Films for n-Channel Thin Film Transistors. *Chem. Mater.* **2009**, *21*, 604–611.

(13) Li, Z.-Q.; Zhang, M.; Liu, B.; Guo, C.-Y.; Zhou, M. Rapid Fabrication of Metal-Organic Framework Thin Film Using in situ Microwave Irradiation and Its Photocatalytic Property. *Inorg. Chem. Commun.* **2013**, *36*, 241-244.

(14) Wade, C. R.; Li, M.; Dincá, M. Facile Deposition of Multicolored Electrochromic Metal-Organic Framework Thin Films. *Angew. Chem. Int. Ed.* **2013**, *52*, 13377-13381.

(15) Rashed, M. A.; Laokroekkiat, S.; Hara, M.; Nagano, S.; Nagao, Y. Fabrication and Characterization of Cross-Linked Organic Thin Films with Nonlinear Mass Densities. *Langmuir* **2016**, *32*, 5917−5924.

(16) Sundberg, P.; Karppine, M. Inorganic–Organic Thin Film Structures by Molecular Layer Deposition: A review. *Beilstein J. Nanotechnol.* **2014**, *5*, 1104–1136.

(17) Zhou, H.; Bent, S. F. Fabrication of Organic Interfacial Layers by Molecular Layer Deposition: Present Status and Future Opportunities. *J. Vac. Sci. Technol. A* **2013**, *31*, 040801–040818.

(18) George, S. M.; Yoon, B.; Dameron, A. A. Surface Chemistry for Molecular Layer Deposition of Organic and Hybrid Organic-Inorganic polymers. *Acc. Chem. Res.* **2009**, *42*, 498–508.

(19) Qian, H.; Li, S.; Zheng, J.; Zhang, S. Ultrathin Films of Organic Networks as Nanofiltration Membranes via Solution-Based Molecular Layer Deposition. *Langmuir* **2012**, *28*, 17803–17810.

(20) Quinn, J. F.; Johnston, A. P. R.; Such, G. K.; Zelikin, A. N.; Caruso, F. Next generation, sequentially assembled ultrathin films: beyond electrostatics. *Chem. Soc. Rev.* **2007**, *36*, 707−718.

(21) Buck, M. E.; Schwartz, S. C.; Lynn, D. M. Super hydrophobic thin films fabricated by reactive layer-by-layer assembly of azlactone-functionalized polymers. *Chem. Mater*. **2010**, *22*, 6319−6327.

(22) Lee, B. H.; Ryu, M. K.; Choi, S. Y.; Lee, K. H.; Im, S.; Sung, M. M. Rapid vapor-phase fabrication of organic–inorganic hybrid super lattices with monolayer precision. *J. Am. Chem. Soc.* **2007**, *129*, 16034−16041.

(23) Laokroekkiat, S.; Hara, M.; Nagano, S.; Nagao, Y. Metal−Organic Coordination Network Thin Film by Surface-Induced Assembly. *Langmuir* **2016**, *32*, 6648−6655.

(24) Such, G. K.; Johnston, A. P. R.; Caruso, F. Engineered hydrogen bonded polymer multilayers: from assembly to biomedical applications. *Chem. Soc. Rev.* **2011**, *40*, 19−29.

(25) Adamczyk, N. M.; Dameron, A. A.; George, S. M. Molecular Layer Deposition of Poly(p-phenyleneterephthalamide) Films Using Terephthaloyl Chloride and p-Phenylenediamine. *Langmuir* **2008**, *24*, 2081–2089.

(26) Du, Y.; George, S. M. Molecular Layer Deposition of Nylon 66 Films Examined Using in situ FTIR Spectroscopy. *J. Phys. Chem. C* **2007**, *111*, 8509–8517.

(27) Peng, Q.; Efimenko, K.; Genzer, J.; Pardsons, G. N. Oligomer Orientation in Vapor-Molecular-Layer-Deposited Alkyl-Aromatic Polyamide films. *Langmuir* **2012**, *28*, 10464–10470.

(28) Yoshida, S.; Ono, T.; Esashi, M. Deposition of Conductivity-Switching Polyimide Film by Molecular Layer Deposition and Electrical Modification using Scanning Probe Microscope. *Micro. Nano Lett.* **2010**, *5*, 321–323.

(29) Yoshida, S.; Ono, T.; Esashi, M. Local Electrical Modification of a Conductivity-Switching Polyimide Film Formed by Molecular Layer Deposition. *Nanotechnology* **2011**, *22*, 335302.

(30) Lee, J. S.; Lee, Y. J.; Tae, E. L.; Park, Y. S.; Yoon, K. B. Synthesis of Zeolite as ordered Multicrystal Arrays. *Science* **2003**, *301*, 818–821.

(31) Prasittichai, C.; Zhou, H.; Bent, S. F. Area Selective Molecular Layer Deposition of Polyurea Films. *ACS Appl. Mater. Interfaces* **2013**, *5*, 13391–13396.

(32) Zhou, H.; Bent. S. F. Molecular Layer Deposition of Functional Thin Films for Advanced Lithographic Patterning. *ACS Appl. Mater. Interfaces* **2011**, *3*, 505–511.

(33) Kohli, P.; Blanchard, G. J. Applying polymer chemistry to interface: Layer-by-layer and spontaneous growth of covalently bound multilayers. *Langmuir* **2000**, *16*, 4655–4661.

(34) Zhou, H.; Toney, M. F.; Bent, S. F. Cross-Linked Ultrathin Polyurea Films via Molecular Layer Deposition. *Macromolecules* **2013**, *46*, 5638−5643.

(35) Loscutoff, P. W.; Zhou, H.; Clendenning, S. B.; Bent, S. F. Formation of Organic Nanoscale Laminates and Blends by Molecular Layer Deposition. *ACS Nano* **2010**, *4* (1), 331–341.

(36) Kim, A.; Filler, M. A.; Kim, S.; Bent, S. F. Layer-by-Layer Growth on Ge (100) via Spontaneous Urea Coupling Reactions. *J. Am. Chem. Soc.* **2005**, *127*, 6123–6132.

(37) Kim, M.; Byeon, M. Bae, J-S.; Moon, S-Y.; Yu, G.; Shin, K.; Basarir, F.; Yoon, T-H.; Park, J-W. Preparation of Ultrathin Films of Molecular Networks through Layer-by-Layer Cross-Linking Polymerization of Tetrafunctional Monomers. *Macromolecules* **2011**, *44*, 7092–7095.

(38) Nalwa, H. S.; Watanabe, T.; Kakuta, A.; Mukoh, A.; Miyata, S. N-Phenylated aromatic polyurea: a new non-linear optical material exhibiting large second harmonic generation and u.v. transparency. *Polymer* **1993**, *34* (3), 657–659.

(39) Karimipour, G.; Kowkabi, S.; Naghiha, A. New Aminoporphyrins Bearing Urea Derivative Substituents: Synthesis, Characterization, Antibacterial and Antifungal Activity. *Braz. Arch. Biol. Technol.* **2015**, *58* (3), 431-442.

(40) Wasielewski, M. R. Photoinduced Electron Transfer in Supramolecular Systems for Artificial Photosynthesis. *Chem. Rev.* **1992**, *92*, 435–461.

(41) Coleman, M. M.; Sobkowiak, M.; Pehlert, G. J.; Painter, P. C. Infrared temperature studies of a simple polyurea. *Macromol. Chem. Phys.* **1997**, *198*, 117–134.

(42) Adam, F.; Oo, W-T. Selective oxidation of benzyl alcohol to benzaldehyde over Co-metalloporphyrin supported on silica nanoparticles. *Appl. Catal. A: Gen*. **2012**, *445– 446*, 252– 260.

(43) Sen, P.; Hirel, C.; Andraud, C.; Aronica, C.; Bretonniere, Y.; Mohammed, A.; Hans Agren, H.; Minaev, B.; Minaeva, V.; Baryshnikov, G.; Lee, H-H.; Duboisset, J.; Lindgren, M. Fluorescence and FTIR Spectra Analysis of *Trans*-A_2B_2-Substituted Di- and Tetra-Phenyl Porphyrins. *Materials* **2010**, *3*, 4446-4475.

(44) Hu, Y.; Goodeal, N.; Chen, Y.; Ganose, A. M.; Palgrave, R. G.; Bronstein, H.; Blunt, M. O. Probing the chemical structure of monolayer covalent-organic frameworks grown via Schiff-base condensation reactions. *Chem. Commun.* **2016**, *52*, 9941-9944.

(45) Graf, N.; Yegen, E.; Gross, T.; Lippitz, A.; Weigel, W.; Krakert, S.; Terfort, A.; Unger, W. E. S. XPS and NEXAFS studies of aliphatic and aromatic amine species on functionalized surfaces. *Surf. Sci.* **2009**, *603*, 2849–2860.

(46) Shimizu, K.; Phanopoulos, C.; Loenders, R.; Abela M. L.; Watts, J. F.; The characterization of the interfacial interaction between polymeric methylene diphenyl diisocyanate and aluminum: A ToF-SIMS andXPS study. *Surf. Interface Anal.* **2010**, *42*, 1432–1444.

Table of Contents (TOC)